

# Waveguiding properties of optical vortex solitons

C. T. Law and X. Zhang

Department of Electrical Engineering and Computer Science, University of Wisconsin—Milwaukee, Milwaukee, Wisconsin 53201

G. A. Swartzlander, Jr.

Department of Physics, Worcester Polytechnic Institute, Worcester, Massachusetts 01609

Received July 16, 1999

An optical vortex soliton induces a graded-index waveguide over an extended propagation distance in a self-defocusing nonlinear optical medium. Using numerical techniques, we determine the waveguide dispersion and optimal size of the guided beam. © 2000 Optical Society of America

OCIS codes: 190.3270, 190.4420, 190.5940.

Optically induced waveguiding effects have long fascinated the laser community,<sup>1</sup> owing partly to potential applications such as all-optical switching and modulation.<sup>2</sup> The proposed photonic applications include modulators and all-optical interconnectable waveguides that take advantage of the unique three-dimensional properties of optical vortex solitons (OVS's).<sup>3–11</sup> As in other light-guiding-light schemes, an optical guiding beam is used to induce a channel that has a nonlinear refractive index that can control a signal beam. Whereas OVS waveguides afford three degrees of freedom, planar devices have also been proposed.<sup>12</sup> Here we describe the waveguiding properties of a channel formed by a dark OVS.

The modeled optical configuration, depicted in the inset of Fig. 1, shows a vortex guiding beam passing through a beam splitter and into a nonlinear cell, a collinear signal beam inside the vortex core, and a detector at the output face of the cell. In general, Kerr materials provide efficient use of the guiding beam, inasmuch as all photons contribute equally to the induced index change,  $\Delta n = |n_2| |E|^2$ , where  $n_2 < 0$  is the nonlinear coefficient of the refractive index and  $|E|^2$  is the local beam intensity. A single OVS, centered at the origin in the transverse  $r, \theta$  plane, is characterized by an envelope function that has a dark core and a harmonic phase:

$$E_v = A(r, z) \exp(im\theta), \quad (1)$$

where the complex amplitude vanishes at the origin for all  $z$ ,  $A(0, z) = 0$ , and  $m$  is a signed integer called the topological charge. Within the envelope, the field oscillates as  $\exp[-i(\omega_v t - k_v z)]$ , where  $\omega_v$  and  $k_v$  are, respectively, the frequency and the wave number of the guiding vortex beam, which is assumed to propagate in the  $z$  direction. A closed-form analytical expression for the amplitude does not exist; however, in the region of the dark vortex core  $A \approx E_\infty \tanh(r/w_v)$ , where  $w_v \approx 1.270 w_{NL}$  is the OVS core size,<sup>3</sup>  $E_\infty$  is the background field amplitude,  $w_{NL} = k_v^{-1} (\Delta n_{\max}/n_v)^{-1/2}$  is a characteristic transverse nonlinear scale length,  $k_v = 2\pi n_v/\lambda_v$  is the wave number at the vortex beam wavelength  $\lambda_v$ , and  $n_v$  and  $\Delta n_{\max} = |n_2| E_\infty^2$  are the linear and maximum nonlinear refractive indices in the medium, respectively. The peak of the induced graded-refractive-index profile is located at the center

of the OVS core. This profile not only provides a guiding channel for the OVS (Ref. 5) but also may confine a signal beam, of wave number  $k_u = 2\pi n_u/\lambda_u$  and electric field  $E_u$ . The refractive-index profile for the guided signal beam may be written as  $n = n_u - C\kappa\Lambda\Delta n_{\max} \tanh^2(r/w_v)$ , where  $\Lambda = (n_u \lambda_v^2)/(n_v \lambda_u^2)$  is a phase-mismatch factor,  $C = 4/(1 + \kappa)$ , and  $\kappa$  is the coupling efficiency between the two beams. The extrema of the refractive-index profile are therefore  $n_u$  and  $n_u - C\kappa\Lambda\Delta n_{\max}$ .

To explore the properties of this OVS waveguide in the paraxial limit, we numerically solved the coupled nonlinear Schrödinger equations for the guide described above:

$$-i \frac{\partial v}{\partial Z} + \nabla_\perp^2 v - C(|v|^2 + \kappa\eta|u|^2)v = 0, \quad (2a)$$

$$-i \frac{k_u}{k_v} \frac{\partial u}{\partial Z} + \nabla_\perp^2 u - \Lambda C(\eta|u|^2 + \kappa|v|^2)u = 0, \quad (2b)$$

where  $\nabla_\perp^2 = \partial^2/\partial X^2 + \partial^2/\partial Y^2$  and where  $v = E_v/E_\infty$  and  $u = E_u/E_0$  are the normalized electric fields of the

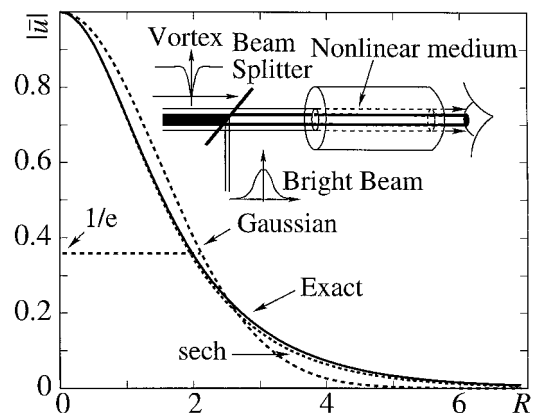


Fig. 1. Transverse profiles of exact (Exact) and trial (sech and Gaussian) eigenmodes within a vortex soliton waveguide have an induced index,  $\Delta n_{\max} = 1.5 \times 10^{-6}$ . The transverse normalization factor is  $w_{NL} = 78 \mu\text{m}$ . The exact eigenmode is determined from Eqs. (4), whereas the trial functions are arbitrary analytical expressions whose size parameters have been optimized to minimize Eq. (6). Inset, experimental setup with a beam splitter to introduce collinear vortex and signal beams within a self-defocusing medium.

guiding vortex and the signal beam, respectively. The signal beam is assumed to be weak:  $\eta = |E_0/\bar{E}_\infty|^2 \ll 1$ . Here we assume that  $E_u$  has a maximum amplitude  $E_0$  at the center of the vortex core. The two fields are coupled through the induced nonlinear refractive index, and we assume a maximum coupling efficiency of  $\kappa = 1$ . Thus we analyze the situation in which the vortex guiding beam has a strong refractive effect on the signal beam but the signal beam has a negligible effect on the guiding beam. The coordinates in Eqs. (2) have also been normalized:  $X = x/w_{\text{NL}}$ ,  $Y = y/w_{\text{NL}}$ ,  $Z = z/z_{\text{NL}}$ , and  $z_{\text{NL}} = 2n_v k_v^{-1} \Delta n_{\text{max}}^{-1}$ . Unless stated otherwise, the examples below assume the following parameters:  $\Delta n_{\text{max}} = 1.5 \times 10^{-6}$ ,  $\lambda_u = \lambda_v = 0.6 \mu\text{m}$ ,  $n_u = n_v = 1$ ,  $w_{\text{NL}} = 78.0 \mu\text{m}$ , and  $z_{\text{NL}} = 127 \text{ mm}$ .

To develop a baseline understanding of the system we consider first the degenerate case,  $k_u = k_v$ , and determine the lowest-order eigenmode of the guided signal. This mode corresponds to the equilibrium signal field in the limit  $z \rightarrow \infty$ , where we may make the ansatz

$$v(R, \theta, Z) = \bar{v}(R) \exp(im\theta) \exp(i2Z), \quad (3a)$$

$$u(R, Z) = \bar{u}(R) \exp(i2\beta Z), \quad (3b)$$

where the last factors in Eqs. (3a) and (3b) account for a nonlinear phase retardation and  $R = (X^2 + Y^2)^{1/2}$  is the normalized radial coordinate. We obtain the equations that govern the amplitudes of the vortex and signal beams by inserting Eqs. (3) into Eqs. (2):

$$2\bar{v} + \frac{1}{R} \frac{\partial}{\partial R} \left( R \frac{\partial \bar{v}}{\partial R} \right) - \frac{m^2}{R^2} \bar{v} - 2|\bar{v}|^2 \bar{v} = 0, \quad (4a)$$

$$2\beta \bar{u} + \frac{1}{R} \frac{\partial}{\partial R} \left( R \frac{\partial \bar{u}}{\partial R} \right) - 2|\bar{v}|^2 \bar{u} = 0. \quad (4b)$$

We may employ numerical methods for two-point boundary problems<sup>13</sup> to determine first  $\bar{v}$  from Eq. (4a) and then  $\bar{u}$  from Eq. (4b). We obtain the exact solution for  $\bar{v}$  by satisfying the conditions  $\bar{v}(R=0) = 0$  and  $\bar{v}(R \rightarrow \infty) = 1$ . For the signal eigenmode, its profile  $\bar{u}$  and eigenvalue (or normalized propagation constant)  $\beta$  are calculated from Eq. (4b) with boundary conditions  $\bar{u}(R=0) = 1$ ,  $\bar{u}(R \rightarrow \infty) = 0$ , and  $d\bar{u}/dR = 0$  at  $R=0$ . The exact numerically obtained eigenmode is shown in Fig. 1 and has an approximate analytic form,  $|\bar{u}| \approx \text{sech}(R/w)$ , where  $w = 1.1506$ . The eigenvalue for the eigenmode is also determined from the collocation method to be  $\beta = 0.3728 \pm 0.0001$ .

To verify the eigenmode solution, we use the ‘‘split-step fast Fourier transform method’’<sup>14</sup> to solve numerically Eqs. (2). We typically use a transverse numerical grid size,  $1024 \times 1024$ , with the vortex core diameter covering at least 20 grid points. In addition to applying the signal eigenmode at the input face on the nonlinear cell, we also test sech and Gaussian trial functions with optimized size parameters (as discussed below). By monitoring the near-axis power and the on-axis intensity over long propagation distances, we are able to distinguish between the guided and radiated propagation modes. To determine the value of the guided power, we integrate the intensity over a

circular aperture of radius  $w_{1/e}$ , where  $w_{1/e}$  is the radial size of the beam in the initial plane ( $z=0$ ) at which the intensity is a factor of  $1/e^2$  times the peak. The power fluctuation percentage is calculated as

$$P_{\%} = 100 \times \left[ 1 - \left( \int_0^{w_{1/e}} |u(r, z)|^2 r dr \right) / \left( \int_0^{w_{1/e}} |u(r, z=0)|^2 r dr \right) \right]. \quad (5)$$

The integration size for the eigenmode is  $w_{1/e} = 1.9499$ , and the values for the other two cases are listed in Table 1. In all three cases, this value is approximately  $w_{1/e} \approx 2$  (or, in physical units, twice the value of  $w_{\text{NL}}$ ) and falls well within the corresponding  $1/e$  vortex core size of  $w_{1/e} = 2.105$ .

The intensity and guided power fluctuations are shown in Fig. 2 for the three trial signal beams. As expected, the exact eigenmode has a constant on-axis intensity and a constant power within the guide; therefore the eigenmode has been verified. In contrast, the sech profile, which appears to closely approximate the eigenmode in Fig. 1, shows noticeable fluctuations in on-axis intensity (<5%) and guide power (<2%) in Fig. 2. Not surprisingly, the Gaussian profile produces even greater fluctuations, reminiscent of a breathing mode. Although the Gaussian trial profile eventually sheds roughly 4% of its power into radiation, it has certain practical advantages. First, most lasers have near-Gaussian profiles, so beam reshaping is not required. Second, any proposed nonlinear device will likely be short in length, to minimize loss through absorption. Over short distances the Gaussian beam tends to focus within the nonlinear waveguide.

Dispersion must be addressed for transmission of broadband or multifrequency signal beams. Inasmuch the induced index has a sech-like profile, modal dispersion is eliminated. Thus the important factors for determining the waveguide bandwidth are the material and waveguide dispersions,  $D_m$  and  $D_w$ , respectively. To determine the waveguide dispersion we must first obtain the optimal values of the signal size parameter  $w$  and the propagation constant  $\beta$  over a range of signal wavelengths  $\lambda_u$ . Furthermore, one may wish to recalculate these values across a range of guiding beam wavelengths,  $\lambda_v$ . The dispersion at a given value of  $\lambda_v$  is calculated with  $D_w = \lambda_u [2c(\pi w_{\text{NL}})^2 n_u]^{-1} \partial^2(\beta_{\text{est}} \lambda_u^2) / \partial \lambda_u^2$ .

**Table 1. Trial Functions for the Nonlinear Guided Wave and the Corresponding Normalized Size  $w$ , Normalized Effective Width  $w_{1/e}$ , and Normalized Propagation Constant  $\beta_{\text{est}}^a$**

Trial Function	$w$	$w_{1/e}$	$\beta_{\text{est}}$
$\text{sech}(R/w)$	1.1506	1.91	0.3740
$\exp[-(R/w)^2]$	2.08	2.08	0.3815

<sup>a</sup>The normalization constant for  $w$  and  $w_{1/e}$  is  $w_{\text{NL}} = 78 \mu\text{m}$ , and for  $\beta_{\text{est}}$  it is  $z_{\text{NL}}^{-1} = (127 \text{ mm})^{-1}$ . Here the OVS waveguide is assumed to have a field profile  $v = \tanh(R/1.27)$ .

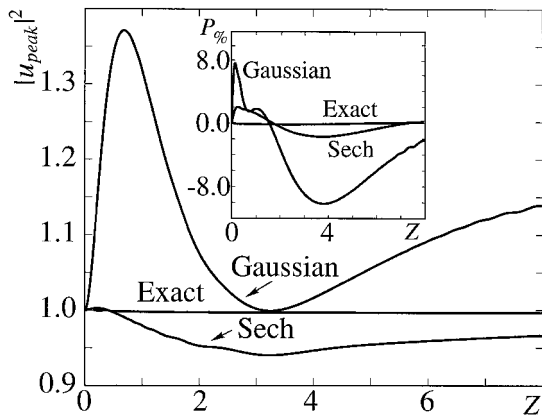


Fig. 2. Variation of signal beam parameters for the profiles in Fig. 1: normalized signal beam peak intensity  $|u_{\text{peak}}|^2$  and percentage change in normalized power  $P\%$  (inset) over an area where the initial signal beam is greater than  $1/e^2$  of its peak intensity versus normalized propagation distance  $Z$ . The longitudinal normalization factor is  $z_{\text{NL}} = 127$  mm.

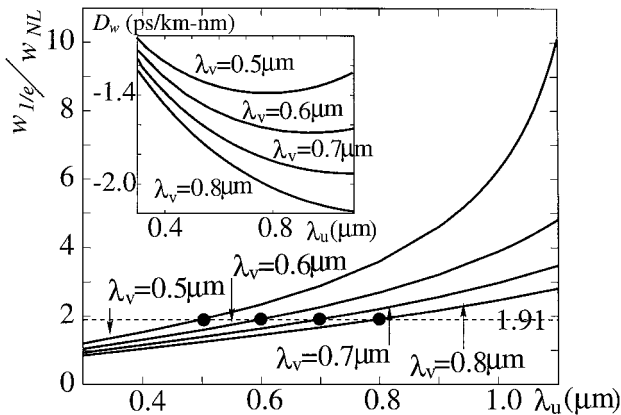


Fig. 3. Normalized optimal width ( $w_{1/e}/w_{\text{NL}}$ ) and waveguide dispersion  $D_w$  (inset) of the sech beam versus its wavelength  $\lambda_u$ . Each curve corresponds to a different guiding beam wavelength  $\lambda_v$  with  $w_{\text{NL}} = 4$   $\mu\text{m}$ , which can be achieved by adjustment of the background intensity.

The optimal size and propagation constant for a trial function  $\bar{u}$  can be determined with the Rayleigh–Ritz variational method,<sup>15</sup> which translates the eigenvalue–eigenmode problem in Eqs. (4) into a functional:

$$\beta_{\text{est}}(w) = \int_0^\infty [R(\partial\bar{u}(w)/\partial R)^2 + 2\Lambda|\bar{v}|^2 R\bar{u}^2(w)]dR \times \left[ \int_0^\infty 2\bar{u}^2(w)RdR \right]^{-1}, \quad (6)$$

where one determines an accurate value of  $\beta$  by varying size parameter  $w$  until the minimum value of  $\beta_{\text{est}}$  is obtained. When this condition is satisfied,  $w$  is optimized. For convenience when minimizing Eq. (6), we approximate the vortex core function with  $\bar{v} = \tanh(R/1.270)$ . The optimal values of  $w$  and  $\beta_{\text{est}}$  for the sech and Gaussian trial functions are listed in Table 1 for the degenerate case,  $k_u = k_v$ . The wavelength-dependent results for the sech trial func-

tion are shown in Fig. 3. To facilitate a comparison with conventional waveguides, we show in Fig. 3  $D_w$  for various  $\lambda_v$  with a fixed value of  $w_{\text{NL}} = 4$   $\mu\text{m}$ . Owing to the phase mismatch  $\Lambda$  between the vortex and signal beams, the light-collecting power of the induced waveguide is weakened as  $\lambda_u$  increases. The signal beam is less confined, and its optimal size increases. For the same reason, a smaller  $\lambda_v$  results in a larger optimal size, whereby  $D_w$  decreases. This trend counteracts the direct dependence of  $D_w$  on  $\lambda_u$  and causes  $|D_w|$  to peak at certain  $\lambda_u$ .

In summary, we have determined that the eigenmode of an OVS waveguide is approximately given by a sech profile whose size is roughly that of the vortex core. The waveguide dispersion ranges from 1 to 2 (ps/km)/nm, depending on the wave numbers of the vortex and guided beams. A Gaussian profile injected into the OVS waveguide will be focused initially and may be useful for use in short nonlinear devices that have compact arrays of OVS waveguides.

C. T. Law was supported by the National Science Foundation CAREER program. G. A. Swartzlander was supported by the Research Corporation as a Cottrell Scholar and by the National Science Foundation as a Young Investigator. C. T. Law's e-mail address is lawc@uwm.edu.

## References

1. G. A. Askaryan, JETP **42**, 1567 (1962) [Sov. Phys. JETP **15**, 1088 (1962)].
2. See K. Blow and G. Stegeman, eds., feature on nonlinear guided waves: physics and applications, J. Opt. Soc. Am. B **14**, 2950–3260 (1997).
3. G. A. Swartzlander, Jr., and C. T. Law, Phys. Rev. Lett. **69**, 2503 (1992).
4. G. A. Swartzlander, Jr., Opt. Lett. **17**, 493 (1992).
5. A. W. Snyder, L. Poladian, and D. J. Mitchell, Opt. Lett. **17**, 789 (1992).
6. J. Christou, V. Tikhonenko, Y. Kivshar, and B. Luther-Davies, Opt. Lett. **21**, 1649 (1995).
7. M. Morin, G. Duree, and G. Salamo, Opt. Lett. **20**, 20 (1995).
8. R. Y. Chiao, I. H. Deutsch, J. C. Garrison, and E. M. Wright, in *Serge Akhmanov: A Memorial Volume*, H. Walther, ed. (Hilger, London, 1992), p. 156.
9. C. T. Law and G. A. Swartzlander, Jr., Chaos Solitons Fractals **4**, 1759 (1994).
10. D. Rozas, C. T. Law, and G. A. Swartzlander, Jr., J. Opt. Soc. Am. B **14**, 3054 (1997).
11. D. Rozas, Z. S. Sacks, and G. A. Swartzlander, Jr., Phys. Rev. Lett. **79**, 3399 (1997).
12. D. R. Andersen, D. E. Hooton, G. A. Swartzlander, Jr., and A. E. Kaplan, Opt. Lett. **15**, 783 (1990); G. A. Swartzlander, Jr., Opt. Lett. **17**, 493 (1992); B. Luther-Davies and Xiaoping Yang, Opt. Lett. **17**, 496 (1992); S. Blair, K. Wagner, and R. McLeod, Opt. Lett. **19**, 1943 (1994).
13. U. Ascher, J. Christiansen, and R. D. Russell, ACM Trans. Math. Software **7**, 209 (1981).
14. J. A. Fleck, Jr., J. R. Morris, and M. D. Feit, Appl. Phys. **10**, 129 (1976).
15. G. Arfken, *Mathematical Methods for Physicists*, 2nd ed. (Academic, New York, 1970), p. 770.